

Conductive Polymer Nanocomposites: From Synthesis to Surface Morphology for Diverse Applications

¹Ms. Hodade Dipali Nagnath, ²Dr. Mohan N Giriya

¹Research Scholar, Department of Physics, Dr. APJ Abdul Kalam University, Indore, MP, India, India
dipalihodade2@gmail.com

²Research Supervisor, Department of Physics, Dr. APJ Abdul Kalam University, Indore, MP, India

Abstract : Conductive polymer nanocomposites have emerged as a significant area of research due to their unique properties and broad application potential across various fields. This study delves into the synthesis, characterization, and surface morphology of these advanced materials, focusing on polyaniline (PANI) nanocomposites for the first time utilized in the search for cadmium sulfate in an aqueous solution. The pioneering effort to produce a polyaniline-CdS nanocomposite involved in-situ oxidative polymerization, revealing crucial insights into the material's physical characteristics. X-ray diffraction (XRD) confirmed the presence of pure nano CdS particles within the PANI matrix, highlighting significant changes in morphology, chemical composition, crystallinity, conductivity, and surface area due to the atypical synthesis techniques. The study reviews the synthesis of polyaniline using both traditional and grafted methods, emphasizing the direct relationship between structure and properties achieved through high-accuracy development processes. Observations demonstrated that PANI/CdS nanocomposites exhibit higher DC conductivity than pure PANI, attributed to the homogeneous intercalation of CdS nanoparticles which enhance the electrical conductivity through a cooperative phenomenon with polyaniline. This investigation not only broadens our understanding of conductive polymer nanocomposites but also paves the way for their innovative use in next-generation technologies, demonstrating their potential to revolutionize various industries.

Keywords: PANI/CdS nano-composite material, Sol-gel, XRD, ZNS, Polyaniline, Polymer, Nano particle

1. INTRODUCTION

The primary focus of this review study was on recent developments in the synthesis and characteristics of polyaniline conducting polymers. Research and development in the synthesis of polyaniline has been examined using a variety of processes, including the traditional technique, ultrasonic, the Fenton process, and substitution on the polyaniline backbone in the form of grafted polyaniline. A direct connection can be seen between the structure and the qualities when using this method of development, which achieves a high level of accuracy in its findings. Polyaniline that has had its structure modified in a number of different ways might produce more interesting outcomes for use in the future. Polyaniline (PANI) is a semi-adaptable bar polymer conducting polymer (CP). Since the mid-1980s, mainstream scholars have scrutinized PANI. Polyaniline stands out among compound semiconductors (CPs) and natural semiconductors due to its easy combination, low environmental effect, and fundamental physics behind doping and de-doping. PANI production is straightforward, but its polymerization and oxidation mechanics are difficult.

Polyaniline has been one of the most studied conducting polymers for 50 years due to its broad scientific foundation. Polyaniline is made by polymerizing aniline monomer and can have three romanticized oxidation states. Leuco-emeraldine is electron-free polyaniline. Imine rather than amine connections indicate fully oxidized pernigraniline. Polyaniline emeraldine base (EB) is neutral. It becomes emeraldine salt (ES) when doped, and an acid protonates the imine nitrogen's. The most practical form of polyaniline is emeraldine base, which is stable at ambient temperature and electrically conductive after doping with acid. Leuco-emeraldine and pernigraniline exhibit low electrical conductivity following acid doping. Sensors and electrochromic devices benefit from polyaniline's color shift in different oxidation states. Despite the importance of color, the best way to make a polyaniline sensor is to use the electrical conductivity changes between oxidation states or doping levels. Polyaniline is usually formed through aniline oxidative polymerization. After dissolving aniline in HCl or another acid (the dopant), ammonium per-sulfate was added drop by drop as the oxidant; the reaction continued for two hours. Special methods and dopants can recover polyaniline powder after polymerization. Dispersibility makes the

powder beneficial for many applications. Three steps may arrange the emeraldine base. The reaction begins with pernigraniline salt (PS) oxidation. In the second stage, the pernigraniline molecule is oxidized to the radicalcation and reduced to the emeraldine salt. The final stage couples this radicalcation with ES salt.

Doped emeraldine salt polyaniline is electrically conductive and ideal for many applications. Electrically leading yarns, antistatic coatings, electromagnetic shielding, and changeable anodes are some examples. The electrochemical arrangement's position is also important. Polyaniline is used to make printed circuit boards (as a last completion) and erosion assurance. This makes polyaniline popular. Polyaniline is commonly created as long chain polymer totals, surfactant (or dopant) settled nanoparticle scatterings, or without stabilizer nano-fiber scatterings, depending on the planned course. Since the late 1990s, polyaniline scattering-cancelling surfactant or dopant has been sold. PANI's unique features, which make it useful in many sectors, have driven interest in its study over the years. This high-performance polymer comes in mass powder, cast films, or filaments and is environmentally friendly and tunable. It's versatile since it's easy to make and mass-produced. Despite the fact that many papers have been published in the last five years, which would indicate that polyaniline is still the subject of much research, most of the fundamental portrayal of polyaniline has occurred in the last 20 years or so and is settled. Despite extensive research on polyaniline, this is true. Polyaniline has an artificially modified -NH aggregate in a polymer chain bordered by phenylene rings. This phenylene-based polymer has an average molecular weight. Monomeric aniline particle 1, 4-coupling can also explain this behavior. NH-gathering proximity causes polyaniline protonation and de-protonation and other physico-concoction properties. Acidic aniline oxidative polymerization produces polyaniline. There are a few polyaniline findings in the literature on aniline polymerization structure and protection.

II. LITERATURE SURVEY

In this Paper Conductive polymers boost light absorption and photocatalytic electrons. CdS-ZnS and CdS-TiO₂ precipitated PANI. Polyaniline improves photocatalysts (CdS, CdS-ZnS and CdS-TiO₂). Measurements included charge transfer, molar ratio, surface form, particle size, diffraction pattern, and heat stability. Nano photo-catalyst PC, CZP, CTP is photo-catalysed. Nanotech enhances photocatalysis. Nanoparticle flaws capture weak CZP and CTP electron kinetics. Recombination reduces CdS-PANI photocatalysis. Photocatalytic water purification CZP, CTP, and CdS-Zn-TiO₂ beat CdS-PANI. PANI attaches photons. High-performance photocatalysts resulted. Nanotechnology

degrades AB-29. Nanotechnology kills AB-29. Cadmium leaching prevents commercial CdS water cleansing. Sold cadmium polyaniline; Polyaniline photocatalysis, stability, reusability; Nano UV-to-IR (i.e., 340–850 nm) (i.e., 340–850 nm); Nanomaterials boost photocatalysis [1].

Cu-Al₂O₃-containing PANI-co-PPy was made in situ. Structure, temperature transition, and morphology were analyzed by FT-IR, XRD, DSC, and HR-TEM (HR-TEM). Novel electrical devices were created by testing AC conductivity and di-electricity at ambient temperature. FT-IR and XRD determined nanoparticle organization and synergy. HR-TEM shows nano-filled copolymer. GTT reduces polymer flexibility, according to DSC. Charge carrier hopping was observed in nanocomposites vs. virgin PANI-co-PPy. Dielectric 5wt% Cu-Al₂O₃ copolymer; nano-filler density improved nanocomposite dielectric characteristics. Al₂O₃ gas-sensing copolymer nanocomposites transmit electrons [2].

Organic pollution harms humans and the environment. Organic contaminants are removed. CdO, Ag-CdO, and Ag-CdO/PANI nanocomposites degraded BPB. Crystal structure, functional groups, morphological change, and efficiency were analyzed by XRD, FTIR, SEM, and UV-Visible spectroscopy. Unlike CdO NPs and Ag-CdO NCs, nanomaterials feature micron-scale grains. PANI-modified Ag-CdO NCs have FT-IR absorption peaks. CdO NPs and Ag-CdO NCs have sharp and strong XRD signals with reducing crystalline diameters. At pH 6, 10 ppm dye, 0.140 g catalyst load, and 210 min irradiation, Ag-CdO/PANI NCs degraded most efficiently [3].

Conductive polymers increase photocatalytic electrons and light absorption. PANI precipitated from CdS, CdS-ZnS, and CdS-TiO₂. PANI polymers improve composite photocatalysts, study finds (CdS, CdS-ZnS and CdS-TiO₂). Charge transfer, molar ratio, surface shape, particle size, diffraction pattern, heat stability, and carrier recombination were measured. Nanocomposites photo-catalyse PC, CZP, and CTP; nanocomposites improve photocatalysis. CZP and CTP entrap nanoparticle surface imperfections due to weak electron kinetics. Charge recombination reduces CdS-PANI photocatalysis. Photocatalysts clean water. CZP and CTP outperformed CdS-PANI because they were compatible with CdS-Zn-TiO₂. PANI absorbs photons. High-performance solar photocatalysts resulted. Nanocomposites degrade AB-29 Dye. Nanocomposites clean AB-29 dyes. Nanoparticle CdS can purify water; however cadmium leaching prevents commercial use. Polyaniline sold cadmium. Comparing polyaniline's photocatalytic activity, stability, and reusability affordable and active nanocomposites; Nano-UV-to-IR (i.e.,

340–850 nm) (i.e., 340–850 nm); Increasing photo-catalyst efficiency demonstrates nanocomposites' promise [4].

In this research, we introduce a new hybrid design from POT-CSA and CdSe-TEA nanoparticles. Structure, morphology, and electricity are investigated. The hybrid material's XRD pattern is cubic, like CdSe nanoparticles. The hybrid films are semiconducting, with a conductivity of 0.1 S.cm⁻² [5].

In this Paper polymerizes in cadmium sulphide following ultrasonic irradiation (CdS). USI manufactures polymer/organic composites. PANI on CdS becomes PANI/CdS. USI nucleates particles. CdS concentration affects PANI/CdS particle size. PANI/CdS particles are created chemically, unlike USI. USI splits PANI/CdS. USI strengthens composite. PANI polymerization on CdS inhibits micro-fibre polymerization. XRD explains USI and validates PANI/CdS. After USI treatment, both materials kept their crystal structures but lost XRD crystallinity. TEM and SEM confirm XRD [6].

PANI study prompted merger. PANI is electrochemical and mechanical. It's vital to limit the reactions that generate PANI and its cheapest cost, then limit its use in nanocomposites with metals, their oxides, and/or carbon to determine what's lacking and broaden its chemistry. Advanced research focused PANI research. PANI's facile preparation and unique features attracted scientists. PANI comprises nanostructured metals, oxides, and carbon (such as carbon nanotubes, graphene, graphene oxide, and reduced graphene oxide). 96Wh/kg power density, 8.88kW/kg energy density; Nano-PANI contributed. Nanostructure and conductivity make PANI a gas sensor. Nano-PANI improves gas sensor performance. This review covers polymer manufacturing, characteristics, nanocomposites, polymerization, and gas sensor applications [7].

PANI and CdS-QDs nanocomposites were morphologically, structurally, optically, and electrically characterized. CdS-PANI nanocomposites precipitated CdS QDs and polyaniline. UV eV is spectroscopy assessed PANI, CdS-PANI nanocomposites, and CdS quantum dots. Quantum dots change PANI's band gap. PANI and its nanocomposites showed 1-D charge transport in DC conductivity measurements. Temperature and CdS content improve CdS-PANI DC conductivity. CdS-PANI nanocomposites' AC conductivity depends on temperature, frequency, and CdS concentration [8].

Ag₂S–CdS was made from silver nitrate and cadmium acetate in thiourea (AC11). In situ polymerization of aniline in AC11 solution yielded PACI. AC11 nanoparticles on PANI formed PACO. PANI, PACI, and PACO counter electrodes for DSCs

(DSSCs). PACI-S was more electro-catalytic than PANI-S and PACO-S. PACI-S DSSCs are photovoltaic compared to PANI-S and PACO-S. PACI-S DSSCs achieved the highest short-circuit current density (12.06 mA/cm²), open-circuit voltage (0.72 V), and fill factor (0.58) [9].

COVID-19 required high-performance energy storage and anti-microbial technology due to energy crises, global warming, and pathogen contamination. Nanocomposites enhance renewable energy and environmental health. In-situ oxidative polymerization generated nanotube-and-quantum-dot MCP nanocomposites. 1-MCP has higher super capacitance than f-MWCNT, 7-MCP, and 5-MCP. Carbon nanotubes and Polypyrrole have high conductivity, surface area, and stability, while cadmium sulphide quantum dots are electro-catalytic. A 24-hour ternary nanocomposite inhibited *S. aureus* and *E. coli*. MCP contains battery and antibacterial properties [10].

This page discusses water pollution adsorbents. Pollution and toxicity have been considered. We evaluate recovery and reuse, toxicity, research limitations, and SFNPs' prospects. SFNPs and derivative composites have unlimited Nano ferrites and their surface-modified composites are studied as waste water adsorbents. This review addresses SFNPs/SFNCs for organic and inorganic pollutant adsorption. Adsorption purifies wastewater simply, effectively, and cheaply. Adsorption isotherm, kinetic, thermodynamic, and mechanistic models are also studied. This report recommends waste water research [11].

Using APS as an oxidant, this study aims to create CdS-based PANI nanocomposites. We also analyze chemical structure, morphology, and electrical properties (FT-IR, XRD, DC conductivity). TEM determines nanoparticle shape and composition. Fore Probe measures CdS composite conductivity. Activation energy is calculated with different cds nanocomposite wt percentages and bulk Polyaniline [12].

Aniline oxidation yielded polyaniline powder. FT-IR spectroscopy revealed absorption peaks at 3498, 2858 cm⁻¹, corresponding to N-H vibrations and C-H expansion of the aromatic ring, as well as quinoid ring stretching vibrations. AFM and SEM measure surface topography and composition. Polyaniline powder pellets' structures were examined using analytical X-ray diffraction. Crystalline lines and three peaks were observed [13].

Polyaniline nanocomposite films were made utilizing aniline, ammonium per sulfate, and cdo. SEM techniques were used to study the development of Pani and Pani/cdo/ZnO composites. Pure Pani and its composites' DC conductivity was measured from 30 to 160°C [14].

Emerging research links microbial extracellular electron transfer (EET) and photo electrochemical processes to circumvent the disadvantages of solitary microbial or photocatalysis treatment; microorganisms use extracellular electron donors for respiration and acceptors to build a respiratory chain. EET-photo electrochemical technologies increase energy conversion efficiency, providing economic and environmental benefits. CdS NPs replace semiconductor photocatalysts. CdS NPs have the electrical conductivity, specific surface area, visible light-driven photocatalysis, and biocompatibility to promote hybrid microbial photo electrochemical processes. This review examines photo electrochemical mechanisms. Future CdS NPs-based microbial-photo electrochemical applications are addressed. This research analyzes the usefulness of developed CdS NPs-bio-hybrids for environmental remediation and clean-energy production [15].

Nano-size CuFe_2O_4 was generated by coprecipitation and 500°C calcination (CF). X-ray diffraction, FTIR, SEM, and photoluminescence spectroscopy on CF-Polyaniline nanocomposite; measuring CF-dielectric PANI's constant at different frequencies and temperatures. In water, CF-PANI eliminated Cr(VI). Contact duration, CF-PANI doses, Cr (VI) ion concentration, pH, and temperature affected Cr(VI) ion removal from aqueous solution. PH 2 absorbed most. Data fit Langmuir isotherm and pseudo-2nd order kinetic models [16].

Co-precipitated $\text{CdS}/\text{CeO}_2/\text{Ag}_3\text{PO}_4$ Photocatalysts were characterized using XRD, BET, SEM-EDX, TEM, UV/Vis, FTIR, and PL. $\text{CdS}/\text{CeO}_2/\text{Ag}_3\text{PO}_4$ has more photocatalytic activity (1:1, 2:1, 3:1, 4:1 molar ratios). PH 4, 10 ppm initial dye concentration, and scavengers are needed to degrade MeO. Scavengers ruin MeO. Photo catalyst removed 93.4% MeO dye. Photocatalytic textile effluent was 70.7%. Also explored was photo catalyst reusability. After four tests, this novel composite preserved 80% of its catalytic efficacy, proving it can destroy MO dye in aquatic environments [17].

Bio-catalytic polymerization is an eco-friendly synthesis process. It uses recyclable, reusable enzymes and yields more than chemical methods. This process is selective, catalytic, efficient, low-energy, etc. under mild circumstances. This method uses organic solvents and enzymes. Enzyme-catalysed polymer has a well-defined structure, while others require undesired steps. Solubility and process ability improve with templates. Polyelectrolyte as a template improves para coupling and may provide doping counterions [18].

III. RESEARCH METHODOLOGY

3.1 Research Methodology

Materials : The materials used were Aniline, Chloroform, Sulphuric Acid (H_2SO_4), Ammonium Persulphate (APS), Cadmium Nitrate ($\text{Cd}(\text{NO}_3)_2$), Methanol, Zinc chloride (ZnCl_2) and Titanium Tetra Isopropoxide (TTIP). All the chemicals were analytical grade and were utilized exactly as they were given to us.

3.1.1 Synthesis of PANI/CdS-PANI/CdS-ZnS-PANI/CdS-TiO₂-PANI Nano Composites : PANI was created via a chemical technique that involved oxidizing aniline in H_2SO_4 with the aid of APS (Ammonium Persulphate). The colour of the solution changed from pale to blue-green and turned to dark green by adding ammonium persulphate to it, indicating that polymerization of aniline into polyaniline occurs swiftly. The operations were performed at low temperatures for the delayed process of polymerization to create the particles in nano size. The following steps were used to make PANI and its different nanocomposites:

3.1.2 Preparation of Polyaniline (PANI) : In 100 mL chloroform, a 0.2 M aniline solution was produced (2.462 M). In 100 mL H_2SO_4 , another APS (0.05 M) solution was produced (1 M) and progressively mixed with the initial solution to polymerize overnight at $4-5^\circ\text{C}$.

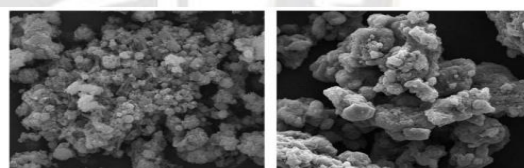


Figure 1: SEM image of pure PANI

3.1.3 Preparation of CdS-PANI Nanocomposite (PC) : PC was made by using a single pot chemical precipitation process to in situ polymerize PANI in CdS nanoparticles. With vigorous stirring, a 100 mL aqueous solution of $\text{Cd}(\text{NO}_3)_2$ (0.085 M) was made and mixed with 50 mL methanol (24.44 M). A 100 mL aniline (0.2 M) solution produced in chloroform (2.462 M) was further mixed with this and stirred for another 60 min. The process was performed for 1 min in an H_2S environment with vigorous stirring and then continued for another 2 h. In a separate vessel, a 0.05 M APS solution was produced in 100 mL H_2SO_4 (1 M). This solution was progressively added to the preceding one and left to polymerize overnight at $4-5^\circ\text{C}$. The finished product was a dark green colour.

3.1.4 Preparation of CdS-ZnS-PANI Nanocomposite (CZP) : With continuous stirring, 50 mL methanol (24.44

M) was dropped into 100 mL aqueous ZnCl_2 (0.15 M). The stirring process was performed for 1 min in an H_2S environment and then followed for about another 2 h, resulting in the change in colour to milky white. In a separate beaker, 100 mL aqueous $\text{Cd}(\text{NO}_3)_2$ (0.085 M) was added dropwise to 50 mL methanol (24.44 M) using a magnetic stirrer. The process was continued by stirring for 1 min in an H_2S environment and then followed for another 2 h. The colour of the solution changed from clear to bright yellow. The two solutions were mixed vigorously for 2 h with vigorous stirring. The solution that resulted was yellow. Next, 100 mL aniline (0.2 M) solution produced in chloroform (2.462 M) was mixed with this reaction mixture and carried out for another 1 h using the stirring method. In a separate vessel, a 0.05 M APS solution was produced in 100 mL H_2SO_4 (1 M). This solution was progressively added to the preceding one and left to polymerize overnight at 4–5 °C. The finished product was a dark green colour.

3.1.5 Preparation of CdS-TiO₂-PANI Nanocomposite (CTP) :

In a typical synthesis, 100 mL aqueous $\text{Cd}(\text{NO}_3)_2$ (0.085 M) was added dropwise with continuous stirring, followed by 50 mL methanol (24.44 M) for 1 min in an H_2S environment using a magnetic stirrer and then followed the same for another 2 h. The colour of the solution changed from clear to yellow. Then, 3.53 mL TTIP (Titanium Tetra Isopropoxide) (0.1 M) was mixed in the dropwise manner to this solution (20 drops per minute), followed by 2 h of stirring. The hue of the solution changed to a faint yellow. Then, 100 mL aniline (0.2 M) solution produced in chloroform (2.462 M) was dropped into this reaction mixture and stirred for 1 h. In a separate vessel, a 0.05 M APS solution was produced in 100 mL H_2SO_4 (1 M). This solution was progressively added to the preceding one and left to polymerize overnight at 4–5 °C. The finished product was a dark green colour. Before drying in the air, all the precipitates were washed numerous times with water and acetone.

3.1.6 Characterization Techniques :

Energy-dispersive X-ray spectroscopy (EDS, JEOL, JSM6510LV, Tokyo, Japan) and Fourier Transform Infrared Spectroscopy were used to examine element analysis (Spectrum 2, PerkinElmer, Waltham, MA, USA). Scanning Electron Microscopy (JEOL, JSM6510LV, Tokyo, Japan) and Transmission Electron Microscopy are used to characterize surface morphology (JEOL, JEM2100, Tokyo, Japan). Powder X-ray diffraction (Miniflex-TM II Benchtop, Rigaku Co-operation, Tokyo, Japan) was used to examine the structural properties. Thermal Gravimetric Analysis was used to determine thermal properties (TGA). UV-Visible Spectroscopy was used to

determine the optical properties (Shimadzu UV-1601, Waltham, MA, USA).

3.1.7 Photocatalytic Experiment : PANI and its nanocomposites (PC, CZP, and CTP) were used in photocatalytic tests to decolorize the dye derivative Acid Blue-29 (AB-29) in visible light. The inner and outer jackets of a standard immersion well photoreactor were employed. A halogen liner lamp was used for irradiation (500 W, 9500 Lumens). In the photocatalytic experiment, 180 mL of the dye solution with the concentration of 0.06 mM and the optimized catalyst dosage (1 gL⁻¹) was stirred in the shady for at least 20 min in the presence of atmospheric oxygen to achieve adsorption–desorption equilibrium between dye and catalyst surface. The initial phase (5 mL) of the solution (0 min) was then removed, and irradiation began. During the irradiation, further sections of samples (5 mL each) were collected at regular intervals and evaluated after centrifugation. Changes in absorption were used to track the decolorization of AB-29 using a UV-vis spectroscopic analysis approach (Shimadzu UV-Vis 1601). The dye concentration was determined using a standard calibration curve based on the dye's absorbance at various known values. It is critical to assess the catalyst's stability and reuse it to put it into practice. The photocatalytic capabilities of the nanomaterials were investigated for five consecutive cycles under similar conditions, using the same amount of catalyst nanomaterials and a fresh solution of dye sample each time.

3.2 Different strategies for the synthesis of metal nanoparticles

Metal nanoparticles could be prepared using two different approaches, which are bottom-up and top-down. In the first approach, the metal nanoparticles are fabricated by starting from metals atoms dissolved in aqueous or organics solution and then deposited under appropriate experimental conditions. In the second approach, the metal nanoparticles are prepared by subdivision of bulk metals usually using physical methods. Considering the above approaches, the methods of synthesis of metal nanoparticles could be classified to six mean methods, as shown in Figure.



Figure 2: Different methods used for the synthesis of metal nanoparticles

The chemical reduction is considered the common method reported in the literature for the synthesis of metal nanoparticles, which are formed by reducing metal salts in the presence of an appropriate reducing agent and a stabilizer usually a special ligand, polymer, or surfactant. The electrochemical methods are widely used in the synthesis of metal nanoparticles. The metal species is dissolved in aqueous or organics solution, then followed by the reduction of metal ions on an appropriate support using cyclic voltametric or a constant reduction potential.

3.2.1 Metal nanoparticles immobilized in polymer matrix : In general, there are three ways to obtaining metal nano particles within polymer matrix, including dispersion, deposition, and immersion. The dispersion method starts with mixing metal precursor with protective polymer and the metal ions are subsequently reduced in the solution. In deposition process, metal precursor which was mixed with protective polymer is deposited onto a substrate.

3.2.2 Sol–gel : Sol–gel methods are also considered as a very promising method for the synthesis of metals nanoparticles. During their synthesis, the experimental conditions including pH, nature of solvent, and temperature strongly effects on properties of the synthesized metal nanoparticles.

3.2.3 Electromagnetic irradiation : The metal nanoparticles could also be prepared using electromagnetic irradiation methods including UV, microwave, ultrasonic, and laser irradiation

3.2.4 Thermal decomposition : Another way for the synthesis of metal nanoparticles is heating volatile metal compounds in organic media or gas phase. The compounds degrade and liberate metal or the corresponding metal oxide in dispersed phase.

3.2.5 Synthesis of nanocrystalline CdS : Nanocrystalline CdS powder has been synthesized by a sol–gel process in which cadmium acetate ($\text{Cd}(\text{CH}_3\text{COO})_2 \cdot 2\text{H}_2\text{O}$) has been used as a parent source for Cd and thiourea ($\text{CH}_4\text{N}_2\text{S}$) has been used as a source of S. For experiment, 3.198 g of cadmium acetate and 1.824 g of thiourea was added into 40 ml of methanol and mixture was stirred vigorously at 60 °C for 1 h (gel formation). After gel formation heating was stopped and the solution was stirred continued until we get a yellow powder. The powder was dried in zone furnace at 300 °C for 30 min to get the nanocrystalline CdS powder having particles of size of 40–50 nm

IV. MATERIALS AND METHODS

4.1 Tensile strength to its absolute limit

The variation in ultimate tensile strength is depicted in Figure 3 as a function of the amount of CdS filler. The final tensile strength found at break varied with increasing filler quantities, and a tendency comparable to this was reported in other places. When compared to clean PVA, the observed values indicate that the tensile strength of polymer nanocomposites is significantly improved across the board for all concentrations of filler. Therefore, it is possible to say that the mechanical properties of composites gain higher reinforcement as a result of the dispersion of nano CdS particles in the matrix. This can be attributed to greater surface area as well as multiple interactions involving various functional groups of the matrix and the filler in the composites. When the amount of CdS in the polymer composite was raised, the tensile strength first improved dramatically and then continued to grow at higher CdS loadings.

Table 1: Range of values for measured thermal properties of PVA/CdS nanocomposites

Temperature,	Units		CdS Content (wt.%)				
CDS Content in PVA (WT.%)	-	-	0	0.5	1.0	1.5	2.0
Heat of Fusion,	ΔH	J/g	40.54	40.89	41.49	37.29	35.72
Percentage	% x_c	%	4.39	5.768	4.572	4.408	4.171
Glass Transition	T _g	°C	81.6	71.3	68.4	71.2	69.2
Melting Temperature	T _m	°C	226.8	179.3	189.2	195.6	199.5

The terms "true stress" and "true strain" are utilized in the computation of toughness.

The embedding of nanoparticles is thought to be responsible for the morphological and structural changes that lead to an increase in toughness. According to the findings of this study,

the composite film with 2% nano CdS had the highest level of toughness.

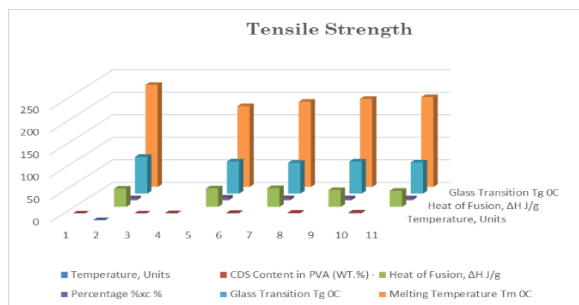


Figure 3 : Range of values for measured thermal properties of PVA/CdS nanocomposites

The significant increase in toughness that was observed in nano-composite films of PVA/CdS in this work is calculated in Table 2 and depicted. When compared to that of pure PVA

film, the nano CdS/PVA film with 2% filler demonstrated the greatest gain in toughness (710 percent more than the pure PVA film). Tensile testing was performed on the samples of PVA and PVA/CdS nano composites in an effort to break them apart. Figure 6 depicts the stress and strain curves of both pure PVA and a nanocomposite film that was created using the nanocomposite. There was a unique pattern that appeared across all of the films, and it was this: the stress level increased with the addition of CdS nanoparticles, which is indicative of the function of these nanoparticles as a reinforcement. The composites exhibit a linear stress–strain character up to the point of failure and plastic deformation. Additionally, the composites confirm a comparable curve shape for both plain and nano filler composites. After being subjected to the treatment, each of the samples exhibited an increase in both their tensile strength and their modulus values.

Table 2. : Effect of nano CdS filler concentration on mechanical properties.

CdS content (wt %)	Young's Modulus (MPa)	% Synergy in Young's Modulus	Toughness (MPa)	% Synergy in toughness	Peak load at break point (N)	UTS (MPa)	Flexural Strength (MPa)
0.0*	33.20	24.6	2.18	174.6	17.7	17.03	4.43
0.5	43.60	31.32	6.67	205.96	21.8	21.97	5.45
1.0	75.50	127.40	13.64	525.69	29	27.00	6.59
1.5	94.30	184.04	10.54	383.49	21.6	27.10	6.75
2.0	91.00	174.10	17.62	708.26	24.5	27.60	7.66

V. RESULTS AND DISCUSSION

5.1 Summary of the parameters extracted from the devices with different cadmium concentrations.

Table 3: Parameters extracted from the devices with different cadmium concentrations

CdCL ₂ Concentration	Resistance (KΩ)	Isc (μA)	Voc (mV)	FF (%)	Efficiency
3.8	4.1	8.9	91	35	0.0389
7	7.9	11	278	32	0.01156
8.9	11.5	38	478	39	0.1098
12	4.6	38	395	49	0.425
14.9	5.8	43	294	37	0.783

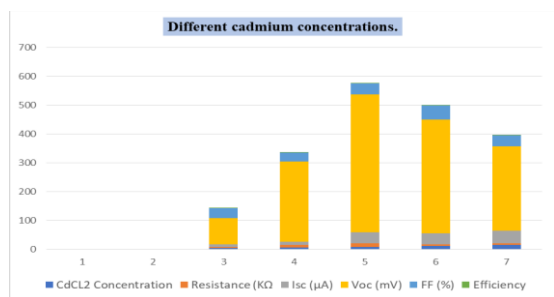


Figure 4: Parameters extracted from the devices with different cadmium concentrations.

The photovoltaic characteristics that were acquired by adjusting the polymerization time, the concentration of

cadmium, and the concentration of dopant. The parameters that were acquired from the devices that contained varied amounts of cadmium are summarized below for your convenience.

5.2 Summary of the parameters extracted from the devices with different polymerization times.

For your convenience, the parameters that were obtained from the devices that contained varying quantities of cadmium are summarized here. These variables were obtained from the devices.

The parameters that were acquired from the devices that exhibited different polymerization periods are summarized in the next paragraphs.

Table 4: Parameters extracted from the devices with different polymerization times.

Time	Resistance (KΩ)	Isc (μA)	Voc (mV)	FF (%)	Efficiency
100	7.8	40	180	16	0.0986
200	11	45	440	40	0.086
300	39	365	520	29	0.78
400	41	105	899	30	0.64
500	52	98	564	35	0.15

The output current (Isc) also increased as the concentration of CdS increased, which may be owing to an increase in defects and, as a result, an increase in light absorption and photon conversion.

band gap that can be tailored to the specifications of the device.

Through the use of photo-electrochemical research, this composite has demonstrated the potential to be utilised in photovoltaic applications. An IPCE value of 11.2% was obtained by photocurrent studies, which revealed a high photon conversion efficiency when exposed to light environments. There will be an improvement in device response if effective solutions for matrix alignment are developed.

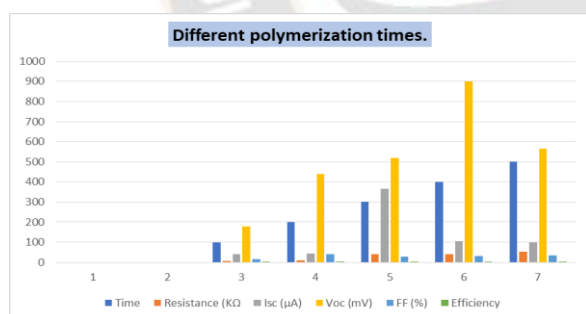


Figure 5: Parameters extracted from the devices with different polymerization times.

Nanoparticles provide a high interfacial surface for charge separation and reduced recombination, whilst polyaniline can be modified to have certain electrical characteristics and a

5.3 The strongest peaks of PANI and CdS which appear in XRD of PANI–CdS(10–50 wt.%) composites

The greatest peaks of PANI and CdS that are found in composites that are formed of PANI and CdS at weight percentages ranging from 10 to 50 are listed below. These peaks were detected in XRD analysis.

Table 5: XRD shows the strongest PANI and CdS peaks

Samples	PANI Peaks			Hexagonal CdS peaks			Cubic CdS peaks		
	2θ deg.	hkl	I/I ₀	2θ deg.	hkl	I/I ₀	2θ deg.	hkl	I/I ₀

10%	25.7	110	100	28.1	101	39	28.1	111	39
20%	25.5	110	100	28.1	101	53	28.1	111	53
30%	25.4	110	100	27.8	101	44	27.8	111	44
40%	25.7	110	100	26.8	002	53	28	111	28
50%	25	110	19	26.6	002	100	27.9	111	27

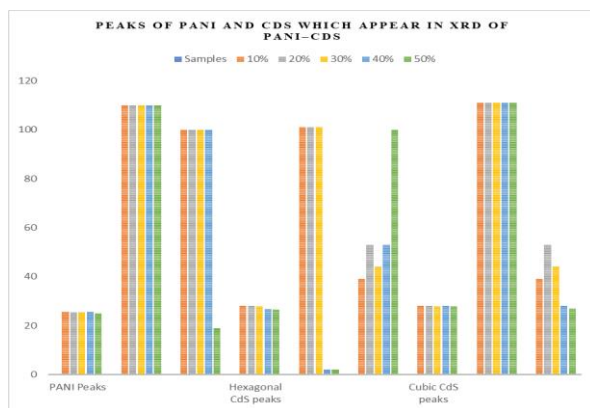


Figure 6: XRD shows the strongest PANI and CdS peaks

The XRD pattern of PANI– CdS (10–50 wt.%) composites show interconnected PANI and CdS peaks. From this pattern, CdS peaks are lower intensity than PANI peaks, but in the sample with 50% CdS, hexagonal and cubic CdS peaks are clearly visible and PANI peak intensity decreases due to CdS concentration, which forms an interlocking structure between CdS nanoparticles and PANI matrix. Table 1 shows the brightest PANI and CdS peaks in PANI–CdS (10–50 wt.%) composite XRD. The high interfacial surface that nanoparticles provide makes it possible to separate charges and reduces the amount of recombination that takes place. This is in contrast to polyaniline, which can be modified to have specific electrical properties and a band gap that can be adjusted according to the requirements of the device. Polyaniline may be altered to have these qualities. Utilizing photo-electrochemical research, it has been established that this composite has the potential to be utilised in applications that are connected to photovoltaics. This potential has been demonstrated by the utilisation of this composite. In the end, an IPCE value of 11.2% was discovered as a consequence of the utilisation of photocurrent experiments, which led to the discovery of a high photon conversion efficiency. As a result of the system being subjected to a variety of light situations, it was discovered that this was the case. It is predicted that there will be an improvement in the device's reaction in the event that effective methods for matrix alignment are

developed. This is why it is anticipated that there will be an improvement.

VI. CONCLUSION

Polyaniline (PANI) is a versatile semi-adaptable bar polymer and conducting polymer that has been extensively studied since the mid-1980s. Its unique characteristics, including simplicity of combination, low environmental impact, and distinct physics governing doping and de-doping, set it apart in the realm of semiconductors. Despite being easy to produce, the polymerization and oxidation mechanisms of PANI pose challenges. Over the past 50 years, PANI has gained popularity as a conducting polymer, with its colour shift in different oxidation states being utilized for sensors and electrochromic devices. Aniline oxidative polymerization is the most common method for PANI production. The resulting powder, recovered through specific methods and dopants, is versatile and applicable in various settings. The past five years have seen continued research on PANI, emphasizing its high-performance qualities, mass production feasibility, and eco-friendly nature. PANI's unique properties make it valuable across sectors, and its electron conjugation can be affected by the chemical composition of inorganic substrates. PANI's application extends to supercapacitors, where its high conductivity, specific capacitance, and various oxidation states make it an ideal electrode material. The electrochemical qualities of PANI-based supercapacitors depend on manufacturing methods and nanostructures. Additionally, PANI has become a prominent sensing material, with various topologies and morphologies contributing to its effectiveness in chemical and biological sensors. The synthesis of PANI with different nanostructures for gas sensors has been explored, showcasing its potential in detecting environmental changes. The crystalline structure of PANI/CdS composites, formed via chemical bath deposition, has been studied, revealing unique properties that make PANI a promising material for further investigation. Overall, PANI's exceptional electrical conductivity, ease of production, and stability in different environments position it as a noteworthy polymer in the field of materials science.

REFERENCES

- [1] Synthesis of Polyaniline Supported CdS/CdS-ZnS/CdS-TiO₂ Nanocomposite for Efficient Photocatalytic Applications, Nida Qutub, Preeti Singh, Suhail Sabir, Khalid Umar, Suresh Sagadevan and Won-Chun Oh, *Nanomaterials* 2022
- [2] Synthesis, Characterization, Conductivity and Gas Sensing Performance of Copolymer Nanocomposites Based on Copper Alumina and Poly(aniline-co-pyrrole) S Sankar M.T. Ramesan, *research square*, 2022
- [3] A promising contender for developing nano-electronic devices.30,300,50,500-tetrabromophenolsulfonphthalein (BPB) under UV-visible light irradiation, Tibebu Alemu, Gutema Taye, Girmaye Asefa, Lemessa B. Merga, *Heliyon*, 2022
- [4] Synthesis of Polyaniline Supported CdS/CdS-ZnS/CdS-TiO₂ Nanocomposite for Efficient Photocatalytic Applications Nida Qutub, Preeti Singh, Suhail Sabir, Khalid Umar, Suresh Sagadevan, and Won-Chun Oh, *Nanomaterials*, 2022
- [5] Novel POT/CdSe blend for optoelectronic applications K. A. Mohammed, K. M. Ziadab, A. S. AL-Kabbi, R. S. Zabibah, *Chalcogenide Letters*, 2022
- [6] Effect of Ultrasonic Irradiation Treatment on the Composites of Polyaniline/Cadmium Sulfide, Ravi V. Ingle, Jupinder Kaur, Prasad E. Lokhande, Vilas A. Tabhane and Habib M. Pathan, *ES Materials and Manufacturing*, 2022
- [7] A Review on Polyaniline: Synthesis, Properties, Nanocomposites, and Electrochemical Applications Abdulwahhab H. Majeed, Leqaa A. Mohammed, Omar G. Hammoodi, Shankar Sehgal, Mustafa A. Alheety, Kuldeep K. Saxena, Safaa A. Dadoosh, Israa K. Mohammed, Mustafa M. Jasim, and N. Ummal Salmaan, *Hindawi International Journal of Polymer Science*, 2022
- [8] Electrical properties of Cadmium Sulfide quantum dots and polyaniline based nanocomposites Akhtar Rasool, Tasneem Zahra Rizvi, Sana Nayab, Zafar Iqbal, *Journal of Alloys and Compounds*, 2022
- [9] Polyaniline/Ag₂S-CdS Nanocomposites as Efficient Electrocatalysts for Triiodide Reduction in Dye-Sensitized Solar Cells Meng Kuo, Tsung-Chia Cheng, Huai-Kai Ye, Tzong-Liu Wang, Tzu-Ho Wu, Chi-Ching Kuo 4 and Rong-Ho Lee, *Catalysts*, 2021
- [10] Synthesis and Application of Nanocomposite Reinforced with Decorated Multi Walled Carbon Nanotube with Luminescence Quantum Dots Jassim Hosny Al Dalaeen, Yashfeen Khan, Anees Ahmad, *Advances in Nanoparticles*, 2021
- [11] Application of Magnetic Nano Particles and their Composites as Adsorbents for Waste Water Treatment: A Brief Review Meenakshi Dhiman, Baljinder Kaur, and Balwinder Kaur, *Materials Research Foundations*, 2021
- [12] Synthesis, D.C. Electrical Conductivity and Activation Energy of Metal Sulphides Doped Polyaniline-Nanocomposite Bhaiswar JB, Meghe DP, Salunkhe MY and Dongre SP, *Der Pharma Chemica*, 2020
- [13] Chemical Synthesis and Characterization of Conducting Polyaniline Salah Abdulla Hasoon, Sally Adel Abdul-Hadi, *Baghdad Science Journal*, 2020
- [14] Electrical properties of polyaniline/Cadmium Oxide/ZnO Nanocomposites Thin Films Jakeer Husain, Rehana Anjum, Shivaraj.G, Gavisiddayya.Mathad, Deepa Pathar, Jaisheel Sagar, Bushara Anjum, *International Research Journal on Advanced Science Hub*, 2020
- [15] Cadmium sulphide nanoparticles-assisted intimate coupling of microbial and photo electrochemical processes: Mechanisms and environmental applications, Guowen Dong, Honghui Wang, Zhiying Yan, Jing Zhang, Xiaoliang Ji, Maozi Lin, Randy A. Dahlgren, Xu Shang, Minghua Zhang, Zheng Chen, *Science of the Total Environment*, *elsevier*, 2020
- [16] Electrical properties of Cadmium Sulfide quantum dots and Copper ferrite-Polyaniline Nanocomposite and its application for Cr (VI) ion removal from aqueous solution N.B. Singha,b, Km Rachna, *Environmental Nanotechnology, Monitoring & Management*, 2020
- [17] Polyaniline supported CdS/CeO₂/Ag₃PO₄ Nanocomposite: An “A-B” type tandem n-n heterojunctions with enhanced photocatalytic activity Abi M. Taddesse, Tigabu Bekele, Isabel Diaz, Abebaw Adgo, *Journal Pre-proof*, 2020
- [18] Synthetic route of PANI (II): Enzymatic method Narendra Pal Singh Chauhan, Masoud Mozafari, *Synthetic route of PANI (II): Enzymatic method*, 2019